

## QUANTITATIVE EVALUATION OF OIL SHALE BASED ON WELL LOG AND 3-D SEISMIC TECHNIQUE IN THE SONGLIAO BASIN, NORTHEAST CHINA

JIANLIANG JIA<sup>(a,b)</sup>, ZHAOJUN LIU<sup>(a)\*</sup>, QINGTAO MENG<sup>(a)</sup>,  
RONG LIU<sup>(a)</sup>, PINGCHANG SUN<sup>(a)</sup>, YONGCHENG CHEN<sup>(c)</sup>

- (a) College of Earth Sciences  
Jilin University  
Changchun 130061, China
- (b) Department of Applied Geosciences and Geophysics  
Montanuniversität Leoben  
A-8700 Leoben, Austria
- (c) SINOPEC Northeast Petroleum Bureau  
Changchun 130056, China

**Abstract.** *The quantitative evaluation of the Upper Cretaceous oil shale has been conducted by abundant testing, log and seismic data from the Songliao Basin in Northeast China. Based on the log-seismic characteristics of oil shale, the technique of log-seismic multi-attributes reconstruction to evaluate single-well oil shale has been adopted. By using the method of log-constrained seismic inversion, the inversion volume of wave impedance, total organic carbon (TOC), and oil yield have been obtained to carry out evaluation of oil shale. According to the evaluation results, the inversion of wave impedance can only be used for qualitative evaluation of the spatial distribution of oil shale. Meanwhile, the inversion of TOC and oil yield can be used not only to evaluate the spatial distribution of oil shale, but also for quantitative evaluation of the quality of oil shale. Hence, the evaluation technique of oil shale was developed combining single-well log evaluation and spatial seismic evaluation, which integrates the quantitative evaluation of oil shale with geophysical technique.*

**Keywords:** *Songliao Basin, the Upper Cretaceous, log technique; seismic technique, quantitative evaluation.*

### 1. Introduction

China has abundant oil shale resources. According to the data of “The National Oil Shale Resource Evaluation of China”, oil shale resources in

---

\* Corresponding authors: e-mail [liuzj@jlu.edu.cn](mailto:liuzj@jlu.edu.cn); [jljia82@yahoo.cn](mailto:jljia82@yahoo.cn)

China were 719.9 billion tonnes in 2006, only second to that of the US. The Songliao Basin has resources of 323.7 billion tonnes, accounting for 45.0 wt% of the region's total [1]. The huge resource potential of oil shale in this basin has not been investigated profoundly.

Oil shale is an emerging type of strategic energy source and has attracted extensive attention in recent years [2–8]. The traditional evaluation of oil shale is based mainly on the determination of oil yield and TOC. Such an approach is constrained by the number and distribution of samples, as well as by testing costs. Because of the predictable defects of this method, log evaluation technique of oil shale was developed. He et al. [9] adopted the curve overlap and  $\Delta\log R$  method for the assessment of oil shale.

Numerous studies have been carried out on the log evaluation of source rock. Beers, Swanson, Fertl and Rieke, Schmoker, Tan, Hertzog et al. [10–15] adopted the gamma-ray log method to identify source rock. Schmoker [16] and Hester [17] used the density log method to determine organic matter content in source rock. Autric [18], Hussain [19] adopted the acoustic and resistivity log prediction method for source rock. Meyer and Nederlof [20], Zhao [21] formulated a linear equation from the correlation diagram of well logs to distinguish source rocks and non-source rocks. Mendelson and Toksoz [22], Fertl and Chilingar [23], Kamel and Mabrouk [24], Xu and Zhu [25] formulated a multiple linear regression equation with multiple log parameters to quantitatively assess source rock. Passey et al. [26] adopted  $\Delta\log R$  technology for the quantitative assessment of source rock. Xu et al. [27], Zhang and Zhang [28], Zhu et al. [29], Kamali and Mirshady [30] applied the  $\Delta\log R$  technology. Huang et al. [31], Huang and Williamson [32], Kamali and Mirshady [30], Kadkhodaie-Ilkhei et al. [33] adopted the artificial neural network algorithm for identification of source rock, and solving the implicit relationship between logs and TOC. Patterson et al. [34] used doppler broadening to examine the relationship between TOC of core samples and a source rocks. The above-mentioned log assessment methods of source rocks use single to multiple parameters and qualitative to quantitative assessment, but the assessment result is limited only to a single well. It is difficult to assess source rocks in the entire basin. Even in the basin with high degree of exploration, high drilling density, and abundant log data, the assessment of source rocks between wells is a challenging task. The spatial assessment of source rocks has been conducted using the seismic method [35–36], in which qualitative prediction of high quality source rocks is performed by the seismic facies and velocity methods. This approach allows roughly estimating the thickness and the range of source rocks and does not allow the quantitative evaluation of source rocks.

## 2. Geological setting

Songliao Basin is located in the northeast of China with an area of  $26 \times 10^4 \text{ km}^2$ . The basin can be divided into 6 first-order tectonic units and 32 second-order tectonic units [37] (Fig. 1). The distribution of oil shale is constrained mainly by the tectonic features, and oil shale is distributed mainly in the southeast uplift zone, northeast uplift zone and central depression zone. The Songliao rift basin has gone through three main tectonic evolutions during Mesozoic era: syn-rift subsidence stage (fault subsidence), post-rift thermal subsidence stage (depression), and rift-shrinking stage (fold) [38]. The oil shale developed during the depression stage.

Development of oil shale in the Songliao Basin is mainly concentrated in the Upper Cretaceous Qingshankou ( $K_2qn$ ) and Nenjiang ( $K_2n$ ) Formations (Fig. 2). The oil shale layers of the 3-D seismic study area (Fig. 1) are at the depth of 1100–1800 m with the monolayer thickness of about 6 m in the Qingshankou Formation deposition, and at the depth of 400–900 m with the monolayer thickness of about 8 m in the Nenjiang Formation deposition (Fig. 2). The Qingshankou Formation is divided into three members based on the lithology. The first member ( $K_2qn_1$ ) incorporated a large lake area

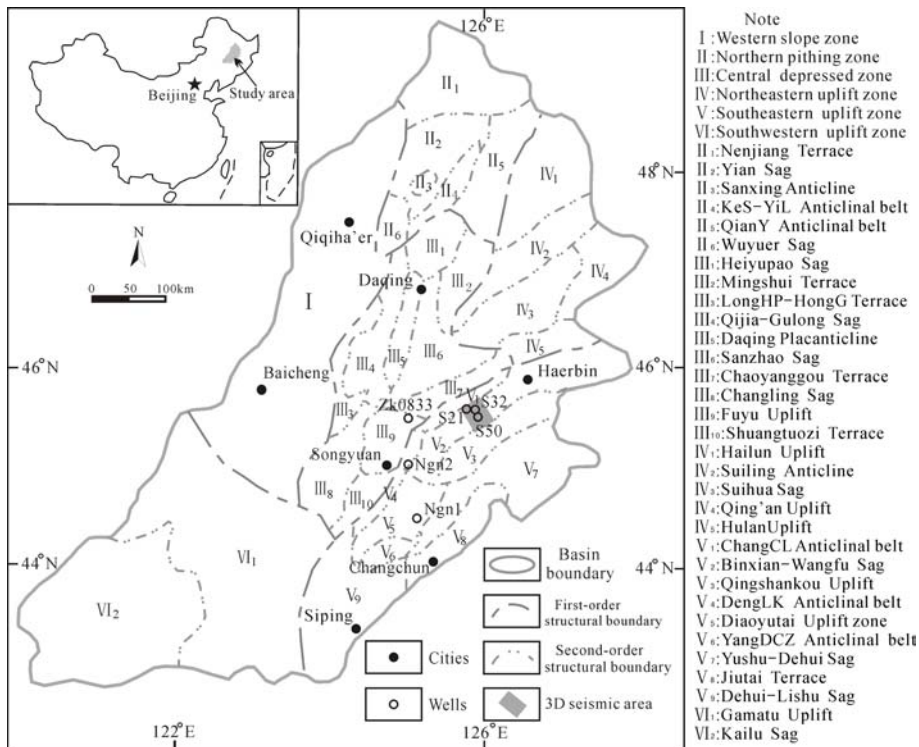
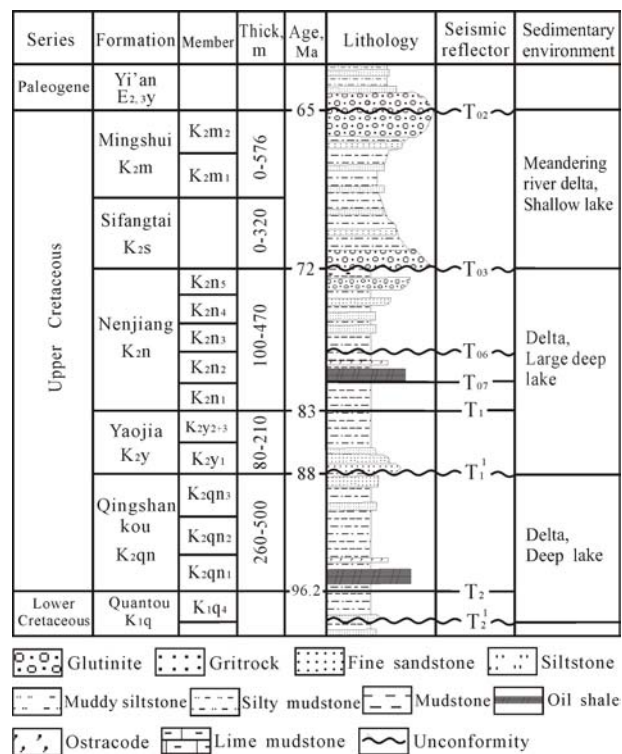


Fig. 1. Zoning map of structural unit of the Songliao basin (modified according to Feng et al., 2010).

during the sedimentary period and developed semi-deep to deep lake facies, with a lithology of mainly gray-black and dark gray mudstone-shale in combination with oil shale, which is mainly formed in semi-deep to deep lake facies. The Nenjiang Formation is divided into five members based on the lithology. A lacustrine transgression phase is reflected by sediments of shallow to semi-deep lake facies. These include grey-black and dark grey mudstones/shales in combination with grey-green siltstones and oil shale that was deposited during the formation period of the first ( $K_{2n1}$ ) and second ( $K_{2n2}$ ) member. The oil shale at the bottom of the second member ( $K_{2n2}$ ) corresponds to the largest lacustrine transgression, during which the Songliao Basin primarily developed and most densely distributed stable oil shale deposits were formed.



Note: The same legend of below lithology columns

Fig. 2. The Upper Cretaceous stratigraphy of Songliao Basin (modified according to Feng et al., 2010 [37]).

### 3. Geophysical evaluation

This paper uses abundant core testing, logging, and 3-D seismic data as a basis. The measured data are from three fully cored wells (Ngn1, Ngn2, and

Zk0833), where each value represents 1 m of core. The 3-D seismic study area is located at the southeast uplift of Binxian-Wangfu Sag, and covers an area of 408 km<sup>2</sup>. Good-quality seismic data serves as a favorable foundation for the exploration of oil shale with geophysical technique.

Based on above data and combined with geophysical methods used by the predecessors on source rock, the technique of log-seismic multi-attributes reconstruct inversion has been applied to carry out the quantitative evaluation of oil shale, to improve efficiency and save costs of the exploration. There are several key steps:

1) Geophysical characteristics of oil shale. This paper analyzes log and seismic response characteristics based on the petrologic characteristics of high organic matter of the oil shale. This constructs a theoretical base to estimate oil shale in the Songliao Basin.

2) Single-well evaluation of oil shale. This paper analyzes the  $\Delta\log R$  technique based on the log response characteristics of oil shale, and constructs the  $\Delta\log R$ -TOC relational model of the Nenjiang Formation. As  $\Delta\log R$  method is unsuitable for use in the Songliao Basin, we mainly adopt the method of log-seismic multi-attributes reconstruction to predict the TOC of single wells.

3) Seismic quantitative evaluation of oil shale. In this paper 3-D seismic data is used. The inversion volume of wave impedance is obtained through the sequence-log constrained seismic inversion method and the inversion volume of TOC. The relationship between TOC and oil yield (measured by the BGMR Fischer Assay method of Royal Dutch Shell Plc) is used to obtain the inversion volume of oil yield and realize the quantitative evaluation of oil shale.

On the basis of above key steps, a technical flowchart for the quantitative evaluation of oil shale with geophysical technique is provided, as shown in Fig. 3.

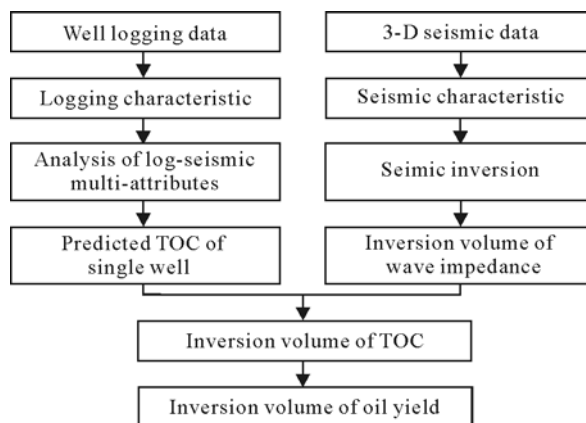


Fig. 3. Evaluation flowchart of geophysical technique of oil shale.

#### 4. Geophysical characteristics of oil shale

The oil shale of the Songliao Basin is mainly composed of lacustrine shale or mudstone, mostly grey-brown, dark grey, and grey-black. It has an organic carbon content of 5.0–10.0 wt% up to 13.6 wt%, and an oil yield of 3.5–8.0 wt% up to 12.1 wt% (Fig. 4).

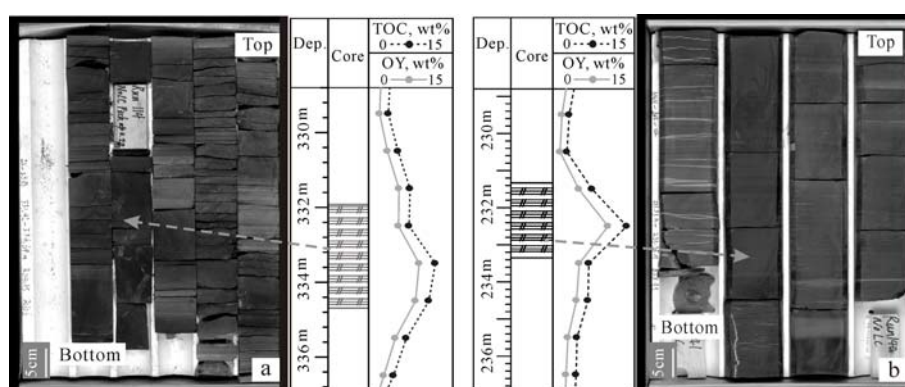


Fig. 4. Petrologic characteristics of oil shale in the Songliao Basin (a) Zk0833 well, K<sub>2</sub>n<sub>2</sub>, grey-brown oil shale; (b) Ngn2 well, K<sub>2</sub>qn<sub>1</sub>, deep grey oil shale.

##### 4.1. Log characteristics of oil shale

The log response characteristics of oil shale depend mainly on the log response to organic matter and rock matrix. The oil shale with high organic matter content has the following characteristics: (1) organic matter has strong radioactivity, and its natural gamma value is higher than that of rock matrix; hence, the oil shale has a high gamma log value; (2) the organic matter is a non-conducting material and its occurrence worsens the conducting property of the rock. Its resistivity is greater than that of rock matrix; thus, the oil shale has a high resistivity log value; (3) the organic matter is the light-weight medium that is not conducive to acoustic wave transmission. The acoustic travel time is greater than that of rock matrix, endowing the oil shale with a log value of high acoustic travel time log value; (4) the organic matter has low density and its density is much lower than that of rock matrix, so the oil shale has a low-density log value; (5) the organic matter has low density, and its hydrocarbon content is considerably higher than that of rock matrix, presenting high-neutron porosity values. Therefore, the log response of oil shale exhibits the “four-high and one-low characteristics”: high-natural gamma, high resistivity, high acoustic travel time, high-neutron porosity, and low density (Fig. 5).

The above-mentioned log response of oil shale can be influenced by the following factors: (1) the radioactive elements in rocks increase the natural

gamma value. For example, the silty thin layers of  $K_2qn_2$  and  $K_2qn_3$  have radioactive uranium, which increases the natural gamma value; (2) the ostracoda beds (Fig. 5, 1502.8 m), sandstone (Fig. 5, 1513 m), and oil shale have similar high resistivity response characteristics; (3) the mudstone layer developed fissures or have gases exhibiting low acoustic velocity, and the log response has a high acoustic travel time log value; (4) the mudstone layer is prone to wall collapse (Fig. 5, 1498 m and 1508 m), and the mud transgression drives the density log value of the undisturbed formation much lower than the normal mudstone. Hence, oil shale exhibits an integrated log response, and its identification is explained by several log methods.

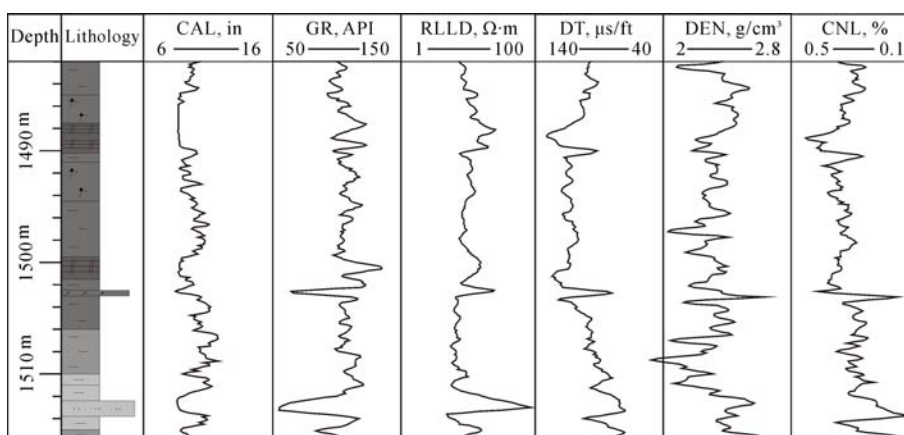


Fig. 5. Log response characteristics of oil shale of well S35 in the Songliao Basin.

#### 4.2. Seismic characteristics of oil shale

The oil shale in the Songliao Basin has the following seismic sedimentary characteristics: (1) The oil shale presents the features of higher frequency, better continuity, and medium-strong amplitude; (2) the seismic reflection structure of oil shale is parallel to subparallel having mainly parallel sedimentation of lacustrine strata in deep water environments. Fig. 6 illustrates the seismic reflection profile across the wells S21-S32 in the Songliao Basin. The profile has four groups of strong reflectors: (1) the seismic event above  $T_2$  shows low-frequency and high-amplitude seismic reflection features. Affected by tectonic fault, the seismic event has low continuity; (2) the seismic event about 1100 ms of well side shows low-frequency, good-continuity and high-amplitude seismic reflection features; (3) the seismic event above  $T_1$  shows double-track seismic reflection features with low frequency, good continuity, and medium-high amplitude; (4) the seismic event above  $T_{07}$  corresponds to the maximum transgressive period of Nenjiang Formation, and shows seismic reflection features with high frequency, medium-high amplitude and good continuity. Thus, the Nenjiang Formation has the



seismic reflection features of high frequency and good continuity and the well calibration, which shows that Nenjiang Formation has thick single layer of oil shale. In view of this, we carry out the log and seismic evaluation mainly on the oil shale of Nenjiang Formation.

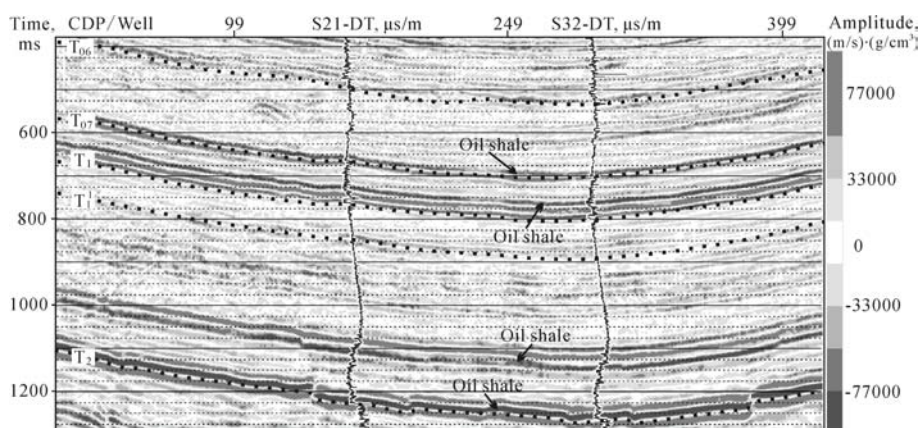


Fig. 6. Seismic response characteristics of oil shale in the Songliao Basin.

Because of seismic resolution constraints, the identification of oil shale on a regular seismic profile can be conducted based only on the drilling calibration result. The seismic reflection feature with strong amplitude is possibly the comprehensive response of the interbedding of mudstone and oil shale. Accurate calibration of the oil shale on the seismic profile is difficult; thus, it is identified by using other seismic methods.

## 5. Single-well evaluation of oil shale

### 5.1. Analysis of $\Delta\log R$ technique

During the logR analysis, three-porosity log curves (acoustic, density and neutron) generally overlay with the resistivity curve. In this study area, the natural gamma response and resistivity curve have good overlay and the oil shale layer has prominent characteristics. Thereby we take gamma/resistivity as the type of curve overlay for  $\Delta\log R$  analysis and assign physical meaning to it. In  $\Delta\log R$  analysis, the combination of log curves reflects the lithology of undisturbed formation correctly and the overlay of log and resistivity curves corresponds to the most prominent log response of oil shale. Only one type of curve cannot be applied blindly.

Figure 7 shows the gamma/resistivity overlay for  $\Delta\log R$  analysis of oil shale in the Nenjiang Formation. The natural gamma response at this well has the most prominent response to oil shale. Although the density curve exhibits good log response at the oil shale layer, it is prone to wall collapse.



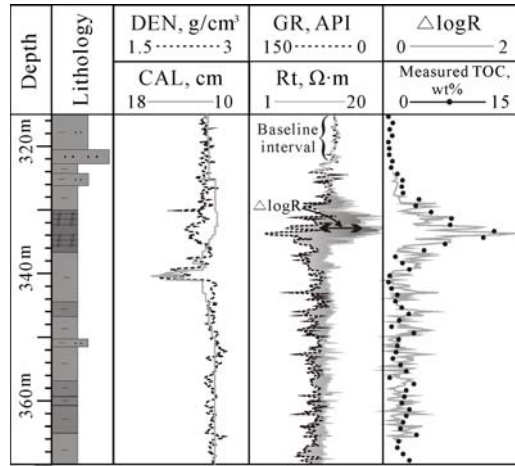


Fig. 7. Analysis of  $\Delta\log R$  of well Zk0833 in the Songliao Basin.

Hence,  $\Delta\log R$  analysis is carried out through gamma/resistivity overlay. Assume that the natural gamma response and resistivity overlay equation for the calculation of  $\Delta\log R$  is:

$$\Delta\log R = \log_{10}(R/R_{\text{baseline}}) + 0.02 \times (GR - GR_{\text{baseline}}), \quad (1)$$

where  $\Delta\log R$  is the curve separation measured in logarithmic resistivity cycles;  $R$ ,  $R_{\text{baseline}}$  present the resistivity log value and the baseline of the overlaid resistivity in  $\Omega\cdot\text{m}$ , respectively;  $GR$ ,  $GR_{\text{baseline}}$  denote the gamma log value and the baseline of the overlaid gamma response in API, respectively; 0.02 is based on the ratio of 50 API per one resistivity cycle mentioned above, an empirical parameter.

According to the baseline of curve overlay,  $GR_{\text{baseline}}$  is 62.03 API and  $R_{\text{baseline}}$  is 5.02  $\Omega\cdot\text{m}$ . These are introduced into equation (1) to obtain  $\Delta\log R$  curve, combined with the measured TOC for linear regression analysis (Fig. 8) and the relational model between the TOC and  $\Delta\log R$  of the Nenjiang Formation from the Songliao Basin is constructed:

$$TOC = 7.3211 \times \Delta\log R + 0.2771, \quad (2)$$

where TOC is the total organic carbon content measured in wt%;  $\Delta\log R$  is the curve separation measured in logarithmic resistivity cycles; 0.2771 is the baseline value of TOC. The "0.2771" is very important to compensate the background value of TOC, and it means that the TOC value is not zero when the  $\Delta\log R$  is zero, which can be proved by measuring TOC from Fig. 8. The TOC and  $\Delta\log R$  show an apparent positive correlation, with a correlation coefficient ( $R^2$ ) of 0.913, indicating that TOC and  $\Delta\log R$  have good correlation and TOC can be predicted by using this relational model.

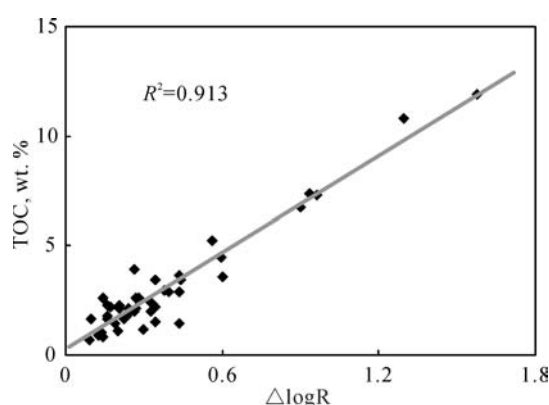


Fig. 8. Correlation diagram of  $\Delta\log R$  vs. measured TOC in the Songliao Basin.

The following two aspects are being paid much attention to during the application of  $\Delta\log R$  technique: (1) the log curve is always influenced by the well environment and cannot reflect the information on undisturbed formation accurately. The accuracy of the log response was monitored before application; (2) the baseline of the  $\Delta\log R$  method represents non-source rocks, and the baseline TOC value is defined as zero value of TOC. However, the TOC of “non-source rock” is not zero, but just lower than the defined value of source rock. Hence, the background value of the TOC curve predicted by the  $\Delta\log R$  method is lower. Generally, a fixed background value is directly added to compensate the baseline value of TOC (e.g. equation (2)). However, in practice the background value may be changed vertically depending on lithology of formation.

## 5.2. Analysis of log-seismic multi-attributes

Regarding to potential issues in the application of  $\Delta\log R$  technique, log-seismic multi-attributes are used to predict TOC. By analyzing the oil shale log and seismic response features, a comprehensive geophysical response is obtained. In this study the TOC is predicted by choosing the prominent log-seismic attributes among the response multi-attributes of oil shale. Additional information regarding the undisturbed formation is incorporated to lay the foundation for improving the precision of TOC prediction. Using log-seismic multi-attributes, the TOC from  $\Delta\log R$  technique is taken as the target curve and carefully chosen log-seismic multi-attributes are integrated to obtain the predicted TOC. This process is divided into two key steps:

(1) Preferred combination of log-seismic multi-attributes: log attributes that are not influenced by the well environment and have good log response are chosen by analyzing the log response characteristics of oil shale. The stepwise regression method is adopted, and the attributes among the log-seismic multi-attributes are chosen based on their degressive error (Table 1).

A preferred combination of log-seismic attributes that have significant influence on the target curve was chosen.

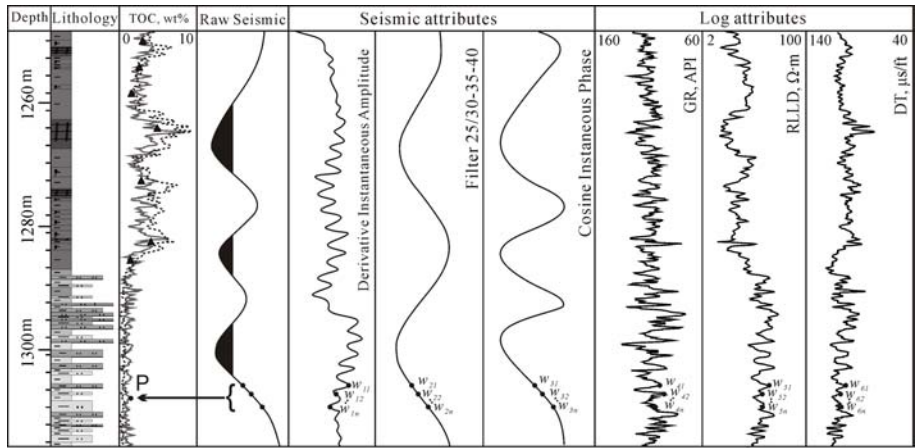
**Table 1. The results of stepwise regression, applied to the TOC prediction problem**

No.	Prediction	Final attributes	Error, %
1	TOC	(GR) <sup>2</sup>	0.8077
2	TOC	log(Rt)	0.2319
3	TOC	1/DT	0.2297
4	TOC	Filter 25/30-35/40	0.2262
5	TOC	Cosine of the instantaneous phase	0.2211
6	TOC	Derivative instantaneous amplitude	0.2189

(2) Integrating log-seismic multi-attributes: the method of multiple stepwise regression analysis is adopted, and the chosen log-seismic attributes (based on their degressive error) are individually integrated into the regression equation. To eliminate the difference in the frequency of the log and seismic attributes, the convolution algorithm is adopted and the single sampling point on the log-seismic attributes is expanded to the adjacent multiple sampling points (Fig. 9), to correlate with the target curve. The weighed average of a group of sampling points on each attributes is taken to calculate a point on the predictive curve, which has almost the same resolution with target curve (well log). The regression equation after convolution is:

$$P = w_0 + w_1 * A_1 + w_2 * A_2 + \dots + w_n * A_n, \tag{3}$$

where  $P$  is the predictive curve;  $*$  represents convolution;  $w_i$  are operators of a specified length;  $A_i$  are attributes [39–41].



— Predicted TOC; ···· TOC from  $\Delta$  logR;  $\blacktriangle$  Measured TOC; P-Predicted point;  $w_i$ -Adjacent multiple sampling points

Fig. 9. Analysis of the log-seismic multi-attributes of well S50 in the Songliao Basin.

To simplify, it was considered to use only four sample values and four log-seismic attributes in equation (3) to predict the TOC. Equation (3) is rewritten as:

$$\begin{bmatrix} \text{TOC}_1 \\ \text{TOC}_2 \\ \text{TOC}_3 \\ \text{TOC}_4 \end{bmatrix} = w_0 + w_1 \begin{bmatrix} E_1 \\ E_2 \\ E_3 \\ E_4 \end{bmatrix} + w_2 \begin{bmatrix} A_1 \\ A_2 \\ A_3 \\ A_4 \end{bmatrix} + w_3 \begin{bmatrix} \text{GR}_1 \\ \text{GR}_2 \\ \text{GR}_3 \\ \text{GR}_4 \end{bmatrix} + w_4 \begin{bmatrix} \rho_1 \\ \rho_2 \\ \rho_3 \\ \rho_4 \end{bmatrix}, \quad (4)$$

where TOC is the total organic carbon content measured in wt%;  $E_i$  are the energy attributes in  $(\text{m/s}) \cdot (\text{g/cm}^3)$ ;  $A_i$  are the amplitude attributes in  $(\text{m/s}) \cdot (\text{g/cm}^3)$ ;  $\text{GR}_i$  are the gamma attributes in API;  $\rho_i$  are the density attributes in  $\text{g/cm}^3$ .

Also, the case of a 3-point operator was taken into consideration, which could be written as follows:

$$w_i = [w_i(-1), w_i(0), w_i(+1)]. \quad (5)$$

Equation (5) was integrated into equation (4), and the matrix is expressed as follows:

$$\begin{bmatrix} \text{TOC}_1 \\ \text{TOC}_2 \\ \text{TOC}_3 \\ \text{TOC}_4 \end{bmatrix} = w_0 + \begin{bmatrix} w_1(0) & w_1(-1) & 0 & 0 \\ w_1(+1) & w_1(0) & w_1(-1) & 0 \\ 0 & w_1(+1) & w_1(0) & w_1(-1) \\ 0 & 0 & w_1(+1) & w_1(0) \end{bmatrix} \begin{bmatrix} E_1 \\ E_2 \\ E_3 \\ E_4 \end{bmatrix} \\ + \begin{bmatrix} w_2(0) & w_2(-1) & 0 & 0 \\ w_2(+1) & w_2(0) & w_2(-1) & 0 \\ 0 & w_2(+1) & w_2(0) & w_2(-1) \\ 0 & 0 & w_2(+1) & w_2(0) \end{bmatrix} \begin{bmatrix} A_1 \\ A_2 \\ A_3 \\ A_4 \end{bmatrix} \\ + \begin{bmatrix} w_3(0) & w_3(-1) & 0 & 0 \\ w_3(+1) & w_3(0) & w_3(-1) & 0 \\ 0 & w_3(+1) & w_3(0) & w_3(-1) \\ 0 & 0 & w_3(+1) & w_3(0) \end{bmatrix} \begin{bmatrix} \text{GR}_1 \\ \text{GR}_2 \\ \text{GR}_3 \\ \text{GR}_4 \end{bmatrix} \\ + \begin{bmatrix} w_4(0) & w_4(-1) & 0 & 0 \\ w_4(+1) & w_4(0) & w_4(-1) & 0 \\ 0 & w_4(+1) & w_4(0) & w_4(-1) \\ 0 & 0 & w_4(+1) & w_4(0) \end{bmatrix} \begin{bmatrix} \rho_1 \\ \rho_2 \\ \rho_3 \\ \rho_4 \end{bmatrix} \quad (6)$$

Items 2, 3, 4 and 5 were reset in equation (6) by turning and simplified as follows:

$$\begin{aligned}
\begin{bmatrix} \text{TOC}_1 \\ \text{TOC}_2 \\ \text{TOC}_3 \\ \text{TOC}_4 \end{bmatrix} &= w_0 + \begin{bmatrix} E_2 & E_1 & 0 \\ E_3 & E_2 & E_1 \\ E_4 & E_3 & E_2 \\ 0 & E_4 & E_3 \end{bmatrix} \begin{bmatrix} w_1(-1) \\ w_1(0) \\ w_1(+1) \end{bmatrix} + \begin{bmatrix} A_2 & A_1 & 0 \\ A_3 & A_2 & A_1 \\ A_4 & A_3 & A_2 \\ 0 & A_4 & A_3 \end{bmatrix} \begin{bmatrix} w_2(-1) \\ w_2(0) \\ w_2(+1) \end{bmatrix} \\
&+ \begin{bmatrix} \text{GR}_2 & \text{GR}_1 & 0 \\ \text{GR}_3 & \text{GR}_2 & \text{GR}_1 \\ \text{GR}_4 & \text{GR}_3 & \text{GR}_2 \\ 0 & \text{GR}_4 & \text{GR}_3 \end{bmatrix} \begin{bmatrix} w_3(-1) \\ w_3(0) \\ w_3(+1) \end{bmatrix} + \begin{bmatrix} \rho_2 & \rho_1 & 0 \\ \rho_3 & \rho_2 & \rho_1 \\ \rho_4 & \rho_3 & \rho_2 \\ 0 & \rho_4 & \rho_3 \end{bmatrix} \begin{bmatrix} w_4(-1) \\ w_4(0) \\ w_4(+1) \end{bmatrix}
\end{aligned} \tag{7}$$

From the equations above, it can be deduced that if single sampling points with (n) attributes are used, there are (n+1) parameters related to the target curve; if multiple sampling points are used, there are ( $Nw_i \times n + 1$ ) parameters related to the target curve, and  $Nw_i$  are the number of operators. With the same number of attributes (n), when the convolution factor algorithm is used, the number of parameters is increased by  $(Nw_i - 1) \times n$ , which is similar to the increase in attributes with lower error; this enables the usage of better attributes in predicting the target curve and thereby improving prediction accuracy.

A combination of 6 log-seismic attributes (GR, Rt, DT, Derivative instantaneous amplitude, Filter 25/30-35-40, and Cosine instantaneous phase) in well S50 is obtained by analyzing the applied stepwise regression, and using a nine-point convolutional operator. The results are shown in Table 1, where each row shows a multi-attribute transform with an increasing number of attributes. The first row shows that the single best attribute is (GR)<sup>2</sup> and a prediction error given by using this attribute is 0.8077%. The second line shows that the best pair of attributes is (GR)<sup>2</sup> and log(Rt), and a prediction error given by using this pair is 0.2319%. Table 1 shows combinations up to 6 attributes.

Figure 9 illustrates the analysis of log-seismic multi-attributes in well S50. The predictive TOC curve is obtained by using the convolution factor algorithm and is validated by the core data measured. The overlay of the predictive TOC, TOC from  $\Delta \log R$  and measured TOC under the same dimension shows that the predictive TOC is much better than the TOC from  $\Delta \log R$  to the measured TOC. The background value of the TOC vertically deviates from the zero line and the baseline changes reasonably, conforming to the vertical variation of organic matter in the undisturbed strata. The quantitative analysis (Fig. 10) shows that the error value of ( $\Delta \text{TOC}_1 = \text{predictive TOC} - \text{measured TOC}$ ) falls between (-0.541) wt% and 0.533 wt%, and the accumulated average error ( $(\sum_{i=1}^n |\Delta \text{TOC}|) / n$ ) is 0.293 wt%. However, the error value of ( $\Delta \text{TOC}_2 = \text{TOC from } \Delta \log R - \text{measured TOC}$ ) is between (-1.109) wt% and 2.082 wt%, and the accumulated average error is

0.995 wt%, which is far more than the  $\Delta\text{TOC}_1$ , so the predictive TOC is rational in comparison to the TOC of  $\Delta\log R$ .

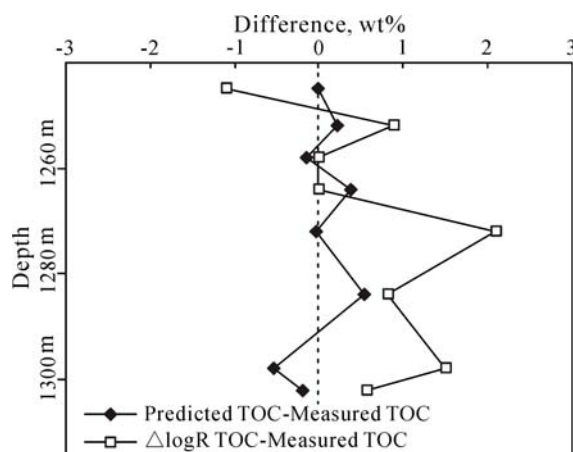


Fig. 10. Analysis of TOC difference of well S50 in the Songliao Basin.

The widespread application of the log-seismic multi-attributes method is limited by data constraints in the study area. However, this method still presents certain advantages: (1) the introduction of seismic attributes of the well site that are not influenced by the well environment to avoid the quality of the log curve to become influenced by the environmental factor of the well; and (2) the good usage of the log-seismic multi-attributes to determine that the shale has better geophysical response, and the adoption of convolution factor algorithm to predict TOC, so that the predictive result responds more accurately to the strata information and allows for a vertically compensated background value of TOC. This conforms to the vertical geological variations of strata in the TOC.

## 6. Seismic quantitative evaluation of oil shale

### 6.1. The log-constrained seismic inversion

Seismic inversion is a common and effective method for interpreting lithology. No report on the interpretation of oil shale using the inversion method has been published because the realization process is subject to numerous constraints, such as the seismic response and seismic resolution of oil shale. The oil shale in the Nenjiang Formation of the Songliao Basin has high-frequency, good-continuity, and medium-high amplitude seismic response characteristics. By drilling, it is determined that the oil shale has thick single layers, which makes identification through the inversion volume possible.

To improve inversion resolution, seismic prediction of oil shale using the seismic inversion method, based on the logging-constraint, was carried out. To make the log and seismic response comparable, the seismic geological horizon is marked during the inversion. This paper uses the seismic synthesis recording method for marking. The seismic synthesis record can be expressed as the convolution of the seismic wavelet and reflection coefficient. The seismic wavelet is obtained through the multi-trace seismic statistical method, and the reflection coefficient is obtained mainly through the acoustic log data. The synthesized seismic trace is compared with the actual seismic trace of well site. The main seismic reflective interface is marked and the synthesis recording of the accurate time-depth relationship is obtained through repeated proper tuning at the given position to realize the marking of the seismic geological horizon. The seismic synthesis recording in Fig. 11 shows that the artificially synthesized seismic trace corresponds very well to the seismic trace of well site. The correlation coefficient is as high as 0.71. Constructing the accurate time-depth relationship is the foundation for log-constrained seismic inversion.

The marking of seismic geological horizon is taken as the sequence constraint. The initial inversion model is constructed by interpolating and extrapolating the log data in the 3-D seismic volume. Setting up the rational inversion parameters and testing them repeatedly at the cross well profile, we evaluated the results within the permissible range. If it exceeds the error limit, the parameters are adjusted and recalculated so that the predicted result becomes reasonable after comparison with the log data. These are then applied to the entire 3-D study area to obtain the inversion volume of wave impedance. Fig. 12 shows one inversion profile crossing wells S21-S32 in the inversion volume. The profile has two apparent abnormal low-velocity belts (brown belts). Through comparison of the drilling lithology, the low-velocity belts are found to be the responses of oil shale in the  $K_2n_1$  and  $K_2n_2$ .

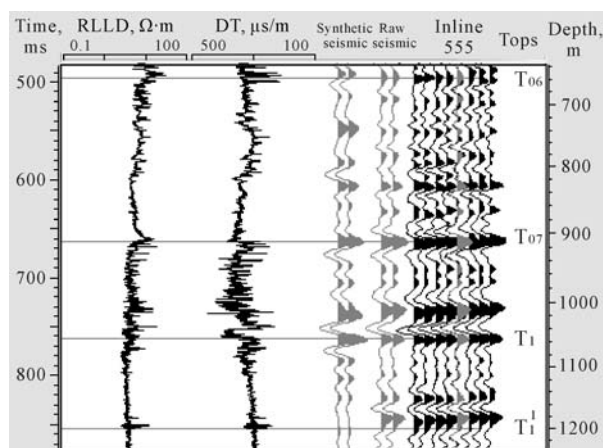


Fig. 11. Seismic synthetic recording of well S21 in the Songliao Basin.



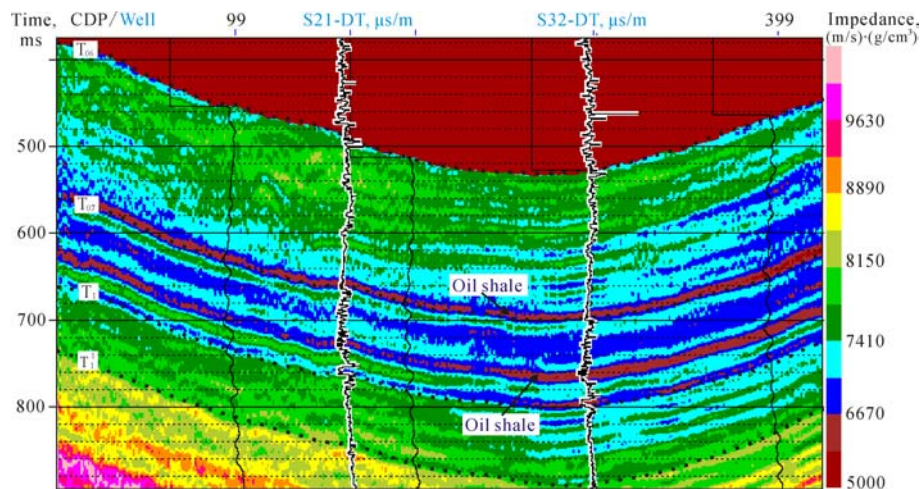


Fig. 12. Inversion profile of wave impedance along a cross section of wells S21-S32 in the Songliao Basin.

The low-velocity belt in the  $K_2n_2$  has good horizontal continuity and stable distribution. The low-  $K_2n_2$  belt in the  $K_2n_1$  has poor continuity and large vertical change in thickness. Hence, the low-velocity belt in the inversion volume has prominent characteristics of spatial distribution, and the spatial distribution of oil shale can be qualitatively predicted by the inversion of low-velocity belt through the log calibration.

The inversion volume of wave impedance is used to predict the spatial distribution of oil shale by displaying relatively low velocity through the adjustment of color marks; this does not achieve the target of quantitative assessment of the spatial distribution of oil shale. To achieve the seismic quantitative evaluation of oil shale, the quantitative parameters like TOC and oil yield of oil shale must be predicted.

## 6.2. Prediction of the inversion volume of TOC

In combining the TOC curves of single-well obtained through log-seismic multi-attributes method and the inversion volume of seismic inversion, we calculate the relationship between the TOC of well site and seismic wave impedance from well side, and then use above relationship to extrapolate from the well to the entire 3-D study area. Finally we obtained the inversion volume of TOC to realize the seismic quantitative evaluation of oil shale.

Spatial quantitative evaluation based on the inversion volume of TOC allows to predict the spatial distribution of oil shale and also enables the quantitative evaluation of oil shale quality. Figure 13 shows the inversion profile of TOC crossing wells S21-S32 in the Songliao Basin. Different colors in the profile represent different TOC values. "Brown" represents the oil shale layers marked by a section with a TOC greater than 5.0 wt%. The

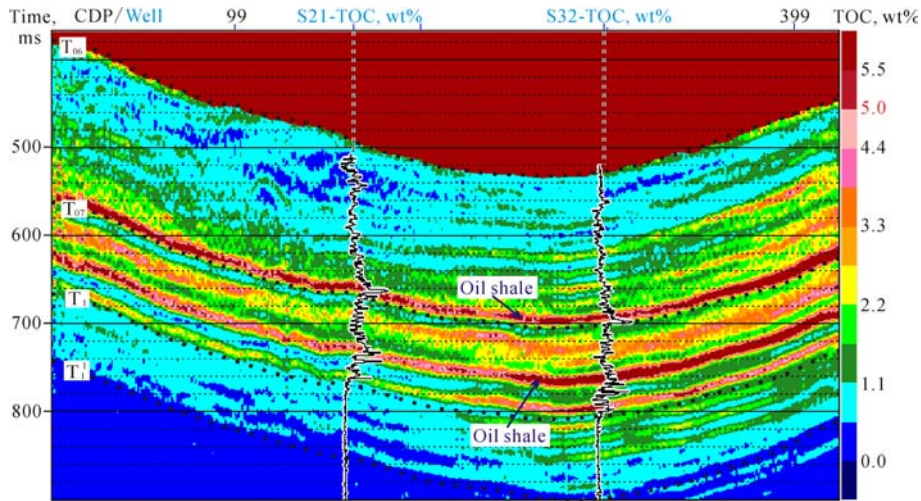


Fig. 13. Inversion profile of TOC along a cross section of wells S21-S32 in the Songliao Basin.

Nenjiang Formation has mainly developed in two oil shale layers. As for the transverse extension, the  $K_{2n2}$  has good continuity, whereas the  $K_{2n1}$  has poor continuity. The TOC inside the oil shale layer changes both transversely and vertically. In Fig. 16, the curves of well-points are the prediction TOC of single-well. Comparing the single-well TOC and inversion TOC of well site shows that the two have good correspondence, which indicates that the seismic method enables the rational prediction of TOC.

### 6.3. Prediction of the inversion volume of oil yield

Oil yield is a direct parameter for quantitative evaluation of the the oil shale and the inversion volume of oil yield must be obtained for the seismic quantitative evaluation of oil shale. By determining the relationship between the TOC and oil yield, the inversion volume of oil yield is obtained through the inversion volume of TOC. To obtain the reliable quantitative relationship between the TOC and oil yield, the data should satisfy the following conditions: (1) to avoid the influence of tectonic factors on oil shale formation, collecting data from wells at different positions of the study area is a more favorable approach; (2) to eliminate model instability resulting from incomplete rules in the section disclosed by the data, collecting data from the continuously cored well is a better technique. The relationship between TOC and oil yield is constructed by 327 measured data from three fully cored wells (Ngn1, Ngn2, and Zk0833) (Fig. 1), as shown below:

$$OY = 0.8015 \times TOC - 0.6645, \quad (8)$$

where OY is the oil yield measured in wt% and TOC is the total organic carbon measured in wt%.

Figure 14 shows a good linear relationship between the TOC and oil yield, and the correlation ( $R^2$ ) is as high as 0.968. When the TOC is 5.0 wt%, the oil yield is about 3.5 wt%. Hence,  $OY > 3.5$  wt% and  $TOC > 5.0$  wt% are taken as the criteria for the quantitative evaluation of oil shale.

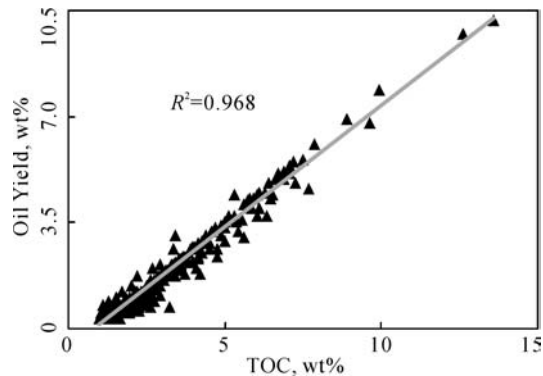


Fig. 14. Correlation diagram of TOC vs. oil yield in the Songliao Basin.

Figure 15 shows the inversion profile of oil yield crossing wells S21–S21 in the Songliao Basin. In the figure, the black layer is the section with an oil yield greater than 3.5 wt%. It can be directly and quantitatively assessed as oil shale. The spatial distribution of oil shale has features similar to the inversion result for the wave impedance and TOC. It is continuous in trans-

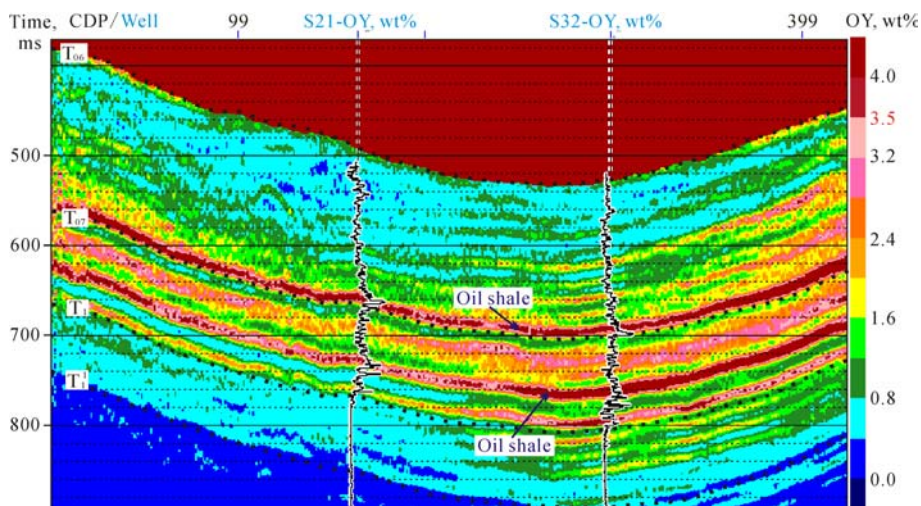


Fig. 15. Inversion profile of oil yield along a cross section of wells S21-S32 in the Songliao Basin.

verse extension and has the distribution features of multi-layers at the vertical direction. The inversion results of oil yield can provide more accurate evaluation. In Fig. 15, the oil yield curve of well and inversion oil yield of well site show better consistency; hence, the inversion result for oil yield is quite rational.

Figure 16 shows the 3-D diagram for the spatial quantitative evaluation of oil shale in the Songliao Basin. In the figure, the layer with oil yield greater than 3.5 wt% is marked as the oil shale. According to the evaluation result, the spatial distribution of oil shale has multi-layers and good continuity. However, the spatial distribution varies among different oil shale layers. The oil shale in the  $K_2n_2$  has good continuity and relatively high oil yield. The fact that  $K_2n_1$  has poor continuity and low oil yield, indicates that the  $K_2n_2$  has better quality of oil shale compared to the  $K_2n_1$ . Meanwhile, the oil shale layer is thick at the bottom of the  $K_2n_2$  and steadily develops in the entire study area, and the inversion of oil yield is either transversely or vertically unstable; the vertical upward inversion changes from low to high and then back to low, and the peak appears at the lower middle part of the oil shale layer. The higher value of oil yield in transverse upward inversion appears at the edges of basin with smaller variations and faults in the secondary tectonic unit. The variation of oil yield from the transverse to the vertical direction indicates that the oil shale represents heterogeneity in spatial

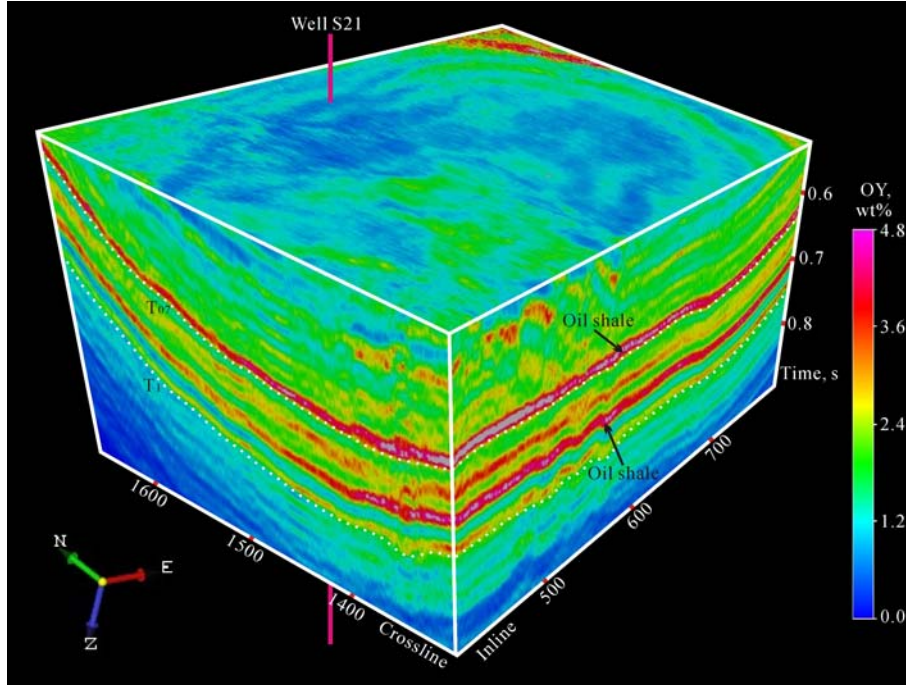


Fig. 16. 3-D diagram for spatial quantitative evaluation of oil shale in the Songliao Basin.



distribution. Hence, the inversion result for oil yield enables quantitative evaluation not only of the spatial distribution of oil shale, but also of the grade of oil shale.

## 7. Conclusion

In this paper, the seismic technique was incorporated into the evaluation system of oil shale, the single-well quantitative evaluation of oil shale with the technique of log-seismic multi-attributes construction was carried out, and the seismic quantitative evaluation of oil shale using the method of logging-constrained seismic inversion was performed. The following conclusions are drawn:

(1) The oil shale of the Songliao Basin exhibits the log response with high natural gamma, high resistivity, high acoustic travel time, high-neutron porosity and low density of the “four-high and one-low characteristics”, and seismic response with higher frequency, better continuity, medium-high amplitude, and parallel to sub-parallel seismic reflection structure.

(2) The  $\Delta\log R$ -TOC relational model for the Nenjiang Formation in the Songliao Basin was constructed and single-well TOC was predicted with log-seismic multi-attributes method. The convolution factor algorithm incorporates  $(Nw_i-1)\times n$  low-error attributes, and the accumulated average error of predictive TOC is 0.293 wt%, which is less than  $\Delta\log R$ . Hence, this method improved the precision of TOC prediction and eliminated the issues caused by the incorrect background values for TOC prediction in the  $\Delta\log R$  method.

(3) A method for the quantitative evaluation of oil shale was proposed using the seismic technique; TOC>5.0 wt% and OY>3.5 wt% was taken as the criteria for the quantitative evaluation of oil shale. According to the evaluation results, the inversion volume of wave impedance obtained through the method of logging-constrained seismic inversion enables the qualitative evaluation of the spatial distribution of oil shale; the inversion volume of TOC and oil yield enables not only the qualitative prediction of the spatial distribution of oil shale, but also the quantitative evaluation of the quality features of oil shale.

The seismic quantitative evaluation of oil shale is supported by abundant log and 3-D seismic data. The prediction accuracy is influenced by the thickness of oil shale and resolution of seismic data. Hence, the technique can be applied in other suitable study areas.

## Acknowledgements

We thank Prof. Dr. R. F. Sachsenhofer and Dr. A. Bechtel for their helpful discussion and suggestions. We are grateful to Dr. S. F. Dai for his constructive and valuable comments. This paper benefited greatly from the

critical remarks by two anonymous reviewers of *Journal Oil Shale*. The research project was financially supported by the National Natural Science Foundation of China (No. 40972076), the National innovation project of production–study–research application of China (No. OSR-01-02), the National Technical Key Special Project of China (No. 2008ZX05018-001-004), the innovation team of Jilin University of China (No. 201004001) and the Graduate Innovation Fund of Jilin University of China (No. 20111043).

## REFERENCES

1. Liu, Z. J., Yang, H. L., Dong, Q. S., Zhu, J. W., Guo, W., Ye, S. Q., Liu, R., Meng, Q. T., Zhang, H. L., Gan, S. C. *Oil Shale in China*. Petroleum Industry Press, Beijing, 2009, 2–3; 157–167 (in Chinese, summary in English).
2. Dyni, J. R. Geology and resources of some world oil-shale deposits. *Oil Shale*, 2003, **20**(3), 193–252.
3. Brendow, K. Global oil shale issues and perspectives. *Oil Shale*, 2003, **20**(1), 81–92.
4. Liu, Z. J., Liu, R. Oil shale resource state and evaluating system. *Earth Science Frontiers*, 2005, **12**(3), 315–323 (in Chinese, summary in English).
5. Liu, Z. J., Dong, Q. S., Zhu, J. W., Guo, W., Ye, S. Q., Liu, R., Zhang, H. L. Oil shale resources and its distribution in China. *China Oil & Gas*, 2007, **14**(3), 26–28.
6. Liu, Z. J., Meng, Q. T., Liu, R. Characteristics and genetic types of continental oil shales in China. *Journal of Palaeogeography*, 2009, **11**(1), 105–114 (in Chinese, summary in English).
7. Reinik, J., Heinmaa, I., Mikkola, J.-P., Kordás, K., Kirso, U. Synthesis of calcium-alumino-silicate hydrates from oil shale ash in different alkaline media. *Oil Shale*, 2010, **27**(1), 47–57.
8. Kavak, O., Connan, J., Erik, N. Y., Yalçın, M. N. Organic geochemical characteristics of Şirnak asphaltites in Southeast Anatolia, Turkey. *Oil shale*, 2010, **27**(1), 58–83.
9. He, J. L., Deng, S. W., Chen, W. L., Jia, Y. K., Gao, J. Q. Evaluation of oil shale in the Southern Songliao Basin using logging techniques. *Journal of Jilin University (Earth Science Edition)*, 2006, **36**(6), 909–914 (in Chinese, summary in English).
10. Beers, R. F. Radioactivity and organic content of some Paleozoic shales. *AAPG Bull.*, 1945, **29**(1), 1–22.
11. Swanson, V. E. Oil yield and uranium content of black shales. *USGS Professional Paper*, 1960, 356-A, 1–44.
12. Fertl, W. H., Rieke, H. H. Gamma ray spectral evaluation techniques identify fractured shale reservoirs and source-rock characteristics. *J. Petrol. Technol.*, 1980, **32**(11), 2053–2062.
13. Schmoker, J. W. Determination of organic-matter content of Appalachian Devonian shales from Gamma-ray logs. *AAPG Bull.*, 1981, **65**(7), 1285–1298.
14. Tan, T. D. Identification of kuchsersits from well logs. *Well Logging Technology*, 1988, **12**(6), 1–11.

15. Hertzog, R., Colson, L., Seeman, O., O'Brien, M., Scott, H., McKeon, D., Wraight, P., Grau, J., Ellis, D., Schweitzer, J., Herron, M. Geochemical logging with spectrometry tools. *SPE Formation Evaluation*, 16792, 1989, **4**(2), 153–162.
16. Schmoker, J. W. Determination of organic content of Appalachian Devonian shales from formation-density logs. *AAPG Bull.*, 1979, **63**(9), 1504–1537.
17. Schmoker, J. W., Hester, T. C. Organic carbon in Bakken Formation, United States portion of Williston Basin. // *AAPG Bull.*, 1983, **67**(12), 2165–2174.
18. Autric, A., Dumensil, P. Resistivity, radioactivity and sonic transit time logs to evaluate the organic content of low permeability rocks. *The Log Analyst*, 1985, **26**(3), 36–45.
19. Hussain, F. A. Source rock identification in the state of Kuwait using wireline logs. *SPE Formation Evaluation*, 15747, 1987, 477–488.
20. Meyer, B. L., Nederlof, M. H. Identification of source rocks on wireline logs by density/resistivity and sonic transit time/resistivity crossplots. *AAPG Bull.*, 1984, **68**(2), 121–129.
21. Zhao, Y. C. The theory and application of logging for source rock evaluation-From the working results in Nanyang and Biyang Depressions. *Earth Science (Journal of China University of Geosciences)*, 1990, **15**(1), 65–74 (in Chinese, summary in English).
22. Mendelson, J. D., Toksoz, M. N. Source rock characterization using multivariate analysis of log data. *SPWLA 26th Annual Logging Symposium*, 1985, paper UU.
23. Fertl, W. H., Chilingar, G. V. Total organic carbon content determined from well logs. *SPE Formation Evaluation*, 15612, 1988, **3**(2), 407–419.
24. Kamel, M. H., Mabrouk, W. M. Estimation of shale volume using a combination of the three porosity logs. *J. Petrol. Sci. Eng.*, 2003, **40**(3–4), 145–157.
25. Xu, S. H., Zhu, Y. Q. Well logs response and prediction model of organic carbon content in source rocks-A case study from the source rock of Wenchang Formation in the Pearl Mouth Basin. *Petroleum Geology & Experiment*. 2010, **32**(3), 290–295. (in Chinese, summary in English).
26. Passey, Q. R., Creaney, S., Kulla, J. B., Moretti, F. J., Stroud, J. D. A practical model for organic richness from porosity and resistivity logs. *AAPG Bull.*, 1990, **74**(12), 1777–1794.
27. Xu, X. H., Huang, H. P., Lu, S. N. A quantitative relationship between well logging information and organic carbon content. *Journal of Jiangnan Petroleum Institute*, 1998, **20**(3), 8–12 (in Chinese, summary in English).
28. Zhang, Z. W., Zhang, L. H. A method of source rock evaluation by well-logging and its application result. *Petroleum Exploration and Development*, 2000, **27**(3), 84–87 (in Chinese, summary in English).
29. Zhu, Z. Y., Liu, H., Li, Y. M. The analysis and application of  $\Delta\log R$  method in the source rock's identification. *Progress in Geophysics*, 2003, **18**(4), 647–649 (in Chinese, summary in English).
30. Kamali, M. R., Mirshady, A. A. Total organic carbon content determined from well logs using  $\Delta\log R$  and Neuro Fuzzy techniques. *J. Petrol. Sci. Eng.*, 2004, **45**(3–4), 141–148.
31. Huang, Z., Williamson, M. A., Fowler, M. G., McAlpine, K. D. Predicted and measured petrophysical and geochemical characteristics of the Egret Member oil source rock, Jeanne d'Arc Basin, offshore eastern Canada. *Mar. Petrol. Geol.*, 1994, **11**(3), 294–306.



32. Huang, Z., Williamson, M. A. Artificial neural network modelling as an aid to source rock characterization. *Mar. Petrol. Geol.*, 1996, **13**(2), 227–290.
33. Kadkhodaie-Ilkchi, A., Rezaee, M. R., Rahimpour-Bonab, H. A committee neural network for prediction of normalized oil content from well log data: An example from South Pars Gas Field, Persian Gulf. *J. Petrol. Sci. Eng.*, 2009, **65**(1–2), 23–32.
34. Patterson, C. D., Quarles, C. A., Breyer, J. A. Possible new well-logging tool using positron Doppler broadening to detect total organic carbon (TOC) in hydrocarbon source rocks. *Radiat. Phys. Chem.*, 2003, **68**(3–4), 523–526.
35. Yu, J. G., Han, W. G., Yu, Z. J., Lu, S. Q., Wang, J. D. Fine interpretation and description of river facies reservoir. *Oil Geophysical Prospecting*, 2005, **40**(3), 318–321 (in Chinese, summary in English).
36. Liu, Z., Chang, M., Zhao, Y., Li, Y. Z., Shen, H. L. Method of early prediction on source rocks in basins with low exploration activity. *Earth Science Frontiers*, 2007, **14**(4), 159–167 (in Chinese, summary in English).
37. Feng, Z. Q., Jia, C. Z., Xie, X. N., Zhang, S., Feng, Z. H., Cross, T. A. Tectono-stratigraphic units and stratigraphic sequences of the nonmarine Songliao basin, northeast China. *Basin Res.*, 2010, **22**(1), 79–95.
38. Liu, Z. J., Wang, D. P., Liu, L., Liu, W. Z., Wang, P. J., Du, X. D., Yang, G. Sedimentary characteristics of the cretaceous in the Songliao Basin. *Acta Geol. Sin-Engl.*, 1993, **6**(2), 167–180.
39. Hampson, D. P., Schuelke, J. S., Quirein, J. A. Use of multiattribute transforms to predict log properties from seismic data. *Geophysics*, 2001, **66**(1), 220–236.
40. Jia, J. L., Liu, Z. J., Chen, Y. C., Fang, S. The technique of log-seismic multi-attributes reconstruction. *Oil Geophysical Prospecting*, 2010, **40**(3), 436–442 (in Chinese, summary in English).
41. Jia, J. L., Liu, Z. J., Chen, Y. C., Fang, S., Yan, L., Sun, P. C. The method of log-seismic multi-attributes density curves to reconstruct inversion and its application. *Journal of Jilin University (Earth Science Edition)*, 2010, **40**(3), 699–706 (in Chinese, summary in English).

*Presented by J. Kann*

Received July 25, 2011